# ULTRA-WIDEBAND RADAR TECHNOLOGY

# ULTRA-WIDEBAND RADAR TECHNOLOGY

Edited by
James D. Taylor, P.E.


CRC Press
Boca Raton London New York Washington, D.C.

**Library of Congress Cataloging-in-Publication Data**

Ultra-wideband radar technology / edited by James D. Taylor.
p. cm.
Includes bibliographical references and index.
ISBN 0-8493-4267-8 (alk.)
1. Radar. 2. Ultra-wideband devices. I. Taylor, James D., 1941-

TK6580 .U44 2000
621.3848—dc21 00-030423



**Visit the CRC Press Web site at www.crcpress.com**


International Standard Book Number 0-8493-4267-8
Library of Congress Card Number 00-030423
6 7 8 9 0

# Preface

*Knowledge is of two kinds. We know a subject ourselves, or we know where we can find information upon it.*

Samuel Johnson (1709–1784)

My first book, *Introduction to Ultra-Wideband Radar Systems,* gave engineers and managers a practical technical theory book about a new concept for remote sensing. *Ultra-Wideband Radar Technology* presents theory and ideas for future systems development and shows the potential capabilities.

Ultra-wideband (UWB) radar systems use signals with a bandwidth greater than 25 percent of the center frequency. In this case, bandwidth means the difference between the highest and lowest frequencies of interest and contains about 95 percent of the signal power. Example waveforms include impulse (video pulse), coded impulse trains, stepped frequency, pulse compression, random noise, and other signal formats that have high effective bandwidths.

UWB radar has advanced since I entered the field in 1987. Several years ago, I received an advertisement for a UWB radar intrusion alarm and bought some as birthday presents for my special ladies. A petroleum distributors' trade magazine described how future gas stations will use UWB communication links and transponders to identify customers and vehicles. While robots fill the tank, the individual account will be properly charged and the transaction completed without the driver leaving the car. Some companies are proposing to build locating systems for factories that will attach a UWB transponder to each container. Personal locating systems are other potential applications. Other companies are designing UWB wireless links to connect homes, offices, and schools.

When I was young, Uncle Scrooge McDuck, a Walt Disney character, had a special watch that computed his income tax by radar. Given the recent commercial development of micropower UWB technology, I expect to see a UWB wristwatch radar advertised soon. It sounds like a great idea for soldiers, policemen, hunters, or anybody who might want to detect hidden persons or objects behind cover. After adding some more technology, follow-on models could calculate your taxes by radar. Gyro Gearloose, Scrooge McDuck's inventor friend, was right on target.

When I organized a session at the 1999 International Ultra-Wideband Conference in Washington, D.C., my speakers reported on UWB radar progress in ground-penetrating radar, airborne SAR systems, automotive radar, and medical imaging. In contrast to the SPIE and IEEE meetings that I usually attend, commercial development issues occupied almost half of the program. The main topic of discussion was about changing the Federal Communications Commission regulations covering low-power UWB sensing and communication systems. It appears that legal issues will be the principal obstacle to future UWB systems development.

Given this background, I think that UWB radar technology will develop along parallel tracks. Commercial low-power short-range systems, using integrated circuit technology for sensing and communications, will be one path. High-power systems for remote fine resolution imaging and sensing will be the other.

Microwatt power impulse radar systems can provide practical solutions to many short-range sensing and communication problems. There is now a strong interest in using UWB signals for short-range wireless interconnection and networking activities. Commercial applications will drive the development of low-power devices once the many regulatory issues are settled. Because UWB signals can provide all-weather sensing and communications over short ranges, it may appear in

smart vehicles and highway systems. I recommend visiting the Ultra-Wideband Working Group web site at www.uwb.org for the latest developments and news.

High-power systems for defense and environmental remote sensing will be the other systems development direction. The American Department of Defense Advanced Research Projects Agency (ARPA) sponsored UWB radar programs during the 1990s. Program objectives included high-resolution sensing and mapping, foliage penetration for imaging hidden objects, and buried mine detection. The annual SPIE sponsored AeroSense conference has been one of the principal forums for reporting UWB radar technology activities and progress.

In my opinion, long-range development goals for high-power systems will include remote environmental and biomass sensing, small target detection using long-duration pulse compression signals and bistatic techniques, and using multiple short range UWB systems to provide high-resolution surveillance for industrial and urban areas. Better uses of polarimetry and signal processing can enhance UWB radar capabilities. Propagation and media characterization studies will help develop better signal processing and imaging techniques.

Discussions with my professional associates indicate that understanding UWB radar requires a new philosophical approach. Because many UWB circuits work with short-duration signals, the steady-state condition is never reached. This requires analyzing the system in the time domain and looking at transient conditions, as opposed to the steady-state frequency response that characterizes many electronic systems.

Fine radar resolution means that targets are much larger than the signal resolution, so they can no longer be considered as point source reflectors. Many of the rules and descriptions used for continuous sinusoidal wave signals cannot be directly applied to UWB radar problems. Concepts such as radar cross section will have new meanings as range resolution becomes smaller than the target.

Chapter 1, "Main Features of Ultra-Wideband (UWB) Radars and Differences from Common Narrowband Radars," was written by Dr. Igor Immoreev of the Moscow State Aviation Institute in Russia. He explains how UWB signals will produce effects not encountered in conventional low-resolution radar. This leads to the concept of signal spectral efficiency. Life is further complicated because fine range resolution turns the target into a series of point returns from scattering centers and creates major signal processing and target detection problems. A direct result of the time-variable UWB antenna and target characteristics is a time-dependent radar range equation.

Chapter 2, "Improved Signal Detection in UWB Radars," by Dr. Igor Immoreev, expands the concepts of Chapter 1. He presents an approach to detecting over-resolved targets by correlating multiple returns over an estimated spatial window about the physical size of the target. This solves the problem of reduced UWB radar returns from numerous scattering centers; however, it will present a new way of considering radar reflection characteristics and target radar cross section specifications.

Chapter 3, "High-Resolution Ultra-Wideband Radars," by Dr. Nasser J. Mohamed, of the University of Kuwait, presents a concept for identifying UWB radar targets. This method involves correlating the series of target returns against a library of known target signals. There is a close relationship with ideas of Chapter 2.

Chapter 4, "Ultra-Wideband Radar Receivers," by James D. Taylor, examines some major theoretical issues in receiver design. This chapter starts with concepts of digitizing and recording impulse signals in a single pass, which is a major problem area building impulse radars for material recognition. Pulse compression is another UWB radar technique that has potential applications where fine range resolution is needed at long ranges. Practical guidance for estimating the bandwidth of UWB signals is given by an explanation of the spectrum of pulse modulated sinewaves. Performance prediction for UWB systems remains a problem area, and the solution may have to be specific to radar systems and waveforms. While the question cannot be answered with a single neat equation, I have provided an approach to performance estimation as a starting point. Chapter 4 is complementary to Chapters 1, 2, and 3.

Chapter 5, "Compression of Wideband Returns from Overspread Targets," by Dr. Benjamin C. Flores and Roberto Vasquez, Jr., of the University of Texas at El Paso, provides a look at how to use pulse compressed signals in radio astronomy. While the ambiguity function was mentioned in Chapter 4, this chapter shows what happens to long-duration pulse-compressed signals when there are time or frequency shifts caused by target motion.

Chapter 6, "The Micropower Impulse Radar," by James D. Taylor and Thomas E. McEwan, examines low-power system technology for short-range applications. Recent advances in integrated circuit technologies will provide a wide variety of short-range sensors and communication systems. Using micropower radar techniques can put radar sensors in places never thought of before.

Chapter 7, "Ultra-Wideband Technology for Intelligent Transportation Systems," by Dr. Robert D. James and Jeffrey B. Mendola, of the Virginia Tech Transportation Center, and James D. Taylor, shows how future smart highway systems can use UWB signals. Short-range sensing and communications are two requirements for watching traffic conditions and then communicating instructions to vehicles. Additionally, we can expect to see some form of radar installed in automobiles and trucks for station maintenance and collision avoidance with other vehicles in traffic. Automotive radar and communications may be a primary UWB development area in the near future; however, it will require a large effort to build smart highways and vehicles. The question of infrastructure design, systems standards, highway control schemes, communication protocols and links, and other issues must be settled before any widespread smart highway system can be built. This chapter raises the potential for vehicle tracing and location, which may raise some serious constitutional privacy issues in a democratic country.

Chapter 8, "Design, Performance, and Applications of a Coherent UWB Random Noise Radar," by Dr. Ram Narayanan, Yi Xu, Paul D. Hoffmeyer, and John O. Curtis, shows how bandwidth alone determines range resolution. Dr. Narayanan and his University of Nebraska associates built and demonstrated a continuous random noise signal radar. By preserving the random noise signal in a delay line, this experimental 1 GHz radar achieved spatial resolution of 15 cm. Such a concept would be potentially valuable for building a stealthy, low probability of intercept radar or for operating at low power levels to avoid interference with other systems.

Chapter 9, "New Power Semiconductor Devices for Generation of Nano- and Subnanosecond Pulses," by Dr. Alexei Kardo-Sysoev, of the Ioffe Physical-Technical Institute in St. Petersburg, Russia, describes the fundamentals of high-power impulse generation. Producing high-power impulse signals involves suddenly moving large amounts of current, which implies special switches that close or open in picoseconds. This chapter explains the theory of drift step recovery diodes and other high-speed switching devices. Dr. Kardo-Sysoev is the head of the Pulse Systems Group of the Ioffe Physical-Technical Institute. His engineers have provided advanced semiconductor switching devices to SRI International and other American organizations.

Chapter 10, "Fourier Series-Based Waveform Generation and Signal Processing in UWB Radar," by Dr. Gurnam S. Gill, of the Naval Post Graduate School in Monterey, California, presents another approach to generating ultra-wideband waveforms. While high-speed switching techniques are a straightforward approach to impulse generation, repeatability remains an issue. There is always a suspicion that each impulse may be slightly different from the others, which will affect signal processing. Generating UWB signals by adding many different waveforms together offers a more flexible approach to building high-power UWB radar systems, especially ones that need a highly accurate and coherent waveform.

Chapter 11, "High-Resolution Step-Frequency Radar," by Dr. Gurnam S. Gill, shows how to build a UWB radar using long-duration narrowband radar signals. Processing many narrowband returns can give the same result as an instantaneous UWB signal. This is an approach to avoiding the regulatory issues that limit high-power UWB system development. Interference with narrowband systems may force the designer to notch out certain restricted frequency bands before the system can be used legally. Dr. Gill develops the theory of using step-frequency waveforms, which transmit many long-duration, narrowband signals and then process them to achieve the effect of a UWB signal.

Chapter 12, "CARABAS Airborne SAR," by Dr. Lars Ulander, Dr. Hans Hellsten, and James D. Taylor, describes a step-frequency UWB radar developed and tested by the Swedish Defence Ministry. The Coherent All Radio Band System (CARABAS) demonstrates how to build a high-resolution SAR using step-frequency radar. CARABAS demonstrated both high-resolution imaging and foliage penetration expected from VHF signals.

Chapter 13, "Ultra-Wideband Radar Capability Demonstrations," by James D. Taylor, describes the state of the art in UWB radar for precision imaging, finding targets hidden by foliage, and detecting buried mines. ARPA-sponsored demonstrations showed the potential of high-power UWB radar as a practical sensing system for military applications. ERIM International, the Lawrence Livermore National Laboratory (LLNL), SRI International, MIT Lincoln Laboratory, and the Army Research Laboratory programs show the capabilities and problems of UWB radar.

Chapter 14, "Bistatic Radar Polarimetry," by Dr. Anne-Laure Germond, of the Conservertoire National des Arts et Metiers in Paris, France, and her colleagues Dr. Eric Pottier, and Dr. Joseph Saillard, presents a new approach to understanding and analyzing bistatic radar signals. Bistatic radar will be an important future technology for detecting small radar cross section targets. Using side-scattered energy for target detection has several potential advantages, including the ability to locate transmitters in protected refuges and move the receiver freely over areas in which it would be dangerous to radiate. Polarimetric radars using orthogonally polarized signals to increase target detection will be a major future radar trend. Analyzing the measured polarization shifts of reflected radar signals may provide a future method for passive target identification. The future of remote sensing may be polarimetric UWB radar.

My special thanks for my collaborators who gave their time and effort to make this book possible. We hope this will stimulate new ideas to advance UWB radar technology.

# Acknowledgments

The editor and authors of this book wish to acknowledge our families, employers, friends, supporters, opponents, and critics. Special thanks to our colleagues who inspired, assisted, and gave their frank considered opinions and suggestions. There are too many to name without unfairly omitting someone, so we must thank you for your contributions this way. We also extend our thanks to the government, industry, and university representatives who made this book possible by supporting and encouraging ultra-wideband radar technology related programs.

My heartfelt thanks to all the writers for working with me and taking my lengthy critiques to heart during the revisions of their chapters. We wanted to make this book unique, useful, and readable.

We thank our families and friends who supported us and provided us the time we needed to prepare this book.

**James D. Taylor**
*January 22, 2000*
*Gainesville, Florida, U.S.A.*

# *In Memoriam*

*Rachel Z. Taylor, 1937–1994*

# Contributors

**John Curtis**
Environmental Laboratory
U.S. Army Waterways Experiment Station
Vicksburg, Mississippi, U.S.A.

**Benjamin C. Flores, Ph.D.**
Department of Electrical and Computer Engineering
University of Texas at El Paso
El Paso, Texas, U.S.A.

**Anne-Laure Germond, Ph.D.**
Chaîre de Physique des Composants
Conservatoire National des Arts et Metiers
Paris, France

**Gurnam S. Gill, Ph.D.**
U.S. Naval Postgraduate School
Monterey, California, U.S.A.

**Hans Hellsten, Ph.D.**
Swedish Defence Establishment (FOA)
Department of Surveillance Radar
Linkoping, Sweden

**Paul Hoffmeyer**
Department of Electrical Engineering
University of Nebraska
Lincoln, Nebraska, U.S.A.

**Igor I. Immoreev**
Doctor of Technical Sciences, and Professor
Moscow State Aviation Institute
Moscow, Russia

**Robert B. James, Ph.D.**
Virginia Tech Transportation Center
Blacksburg, Virginia, U.S.A.

**Alexi F. Kardo-Sysoev**
Doctor of Physico-Mathematical Sciences
Ioffe Physical-Technical Institute
St. Petersburg, Russia

**Thomas E. McEwan, MSEE**
McEwan Technologies LLC
Pleasanton, California, USA

**Jeffrey B. Mendola, MS**
Virginia Tech Transportation Center
Blacksburg, Virginia, U.S.A.

**Nasser J. Mohamed, Ph.D.**
Electrical Engineering Department
University of Kuwait
Safat, Kuwait

**Ram Narayanan, Ph.D.**
Department of Electrical Engineering
University of Nebraska
Lincoln, Nebraska, U.S.A.

**Eric Pottier, Ph.D.**
UPRES-A CNRS 6075 Structures Rayonnantes
Laboratoire Antennes et Télécommunications
Université de Rennes 1
Rennes, France

**Joseph Saillard, Ph.D.**
Ecole Polytechnique de l'Université d Nantes
Nantes, France

**James D. Taylor, MSEE, P.E.**
J.D. Taylor Associates
Gainesville, Florida, U.S.A.

**Lars Ulander, Ph.D.**
Swedish Defence Establishment (FOA)
Department of Surveillance Radar
Linkoping, Sweden

**Roberto Vasquez, Jr.**
Raytheon Electronic Systems
Bedford, Massachusetts

**Yi Xu, Ph.D.**
Department of Electrical Engineering
University of Nebraska
Lincoln, Nebraska, U.S.A.

# About the Editor

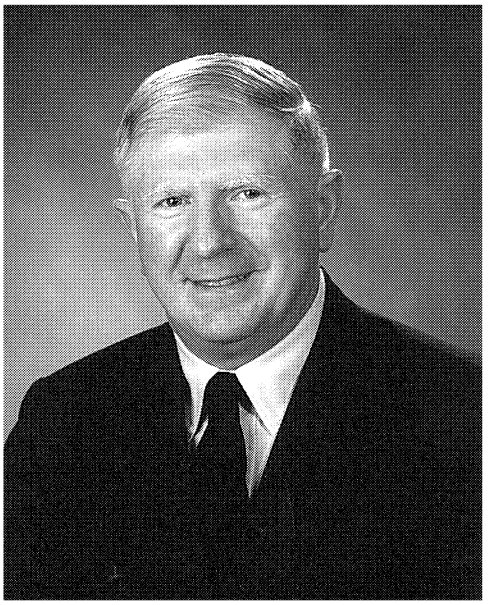

James D. Taylor was born in Tifton, Georgia, in 1941, and grew up in North Carolina and Maryland. After earning his BSEE degree from the Virginia Military Institute in 1963, he entered active duty in the U.S. Army as an artillery officer. In 1968, he transferred to the U.S. Air Force as a research and development electronics engineer and worked for the Central Inertial Guidance Test Facility at Holloman Air Force Base, New Mexico, until 1975. He earned his MSEE in guidance and control theory from the Air Force Institute of Technology at Wright-Patterson AFB, Ohio, in 1977. From 1977 to 1981, he was a staff engineer at the Air Force Wright Aeronautical Laboratories Avionics Laboratory. From 1981 to 1991, he served as a staff engineer in the Deputy for Development Planning at the Electronic Systems Division at Hanscom Air Force Base, Massachusetts.

Upon retiring from the Air Force in 1991, he worked as a consultant to TACAN Aerospace Corp. in San Diego, California, and edited *Introduction to Ultra-Wideband Radar Systems* for CRC Press. He has actively participated in PIERS symposiums radar workshops since 1998 and presented short courses in ultra-wideband radar in America, Italy, and Russia.

His professional achievements include Professional Engineer registration from Massachusetts in 1984. He is a senior member of the Institute of Electrical and Electronics Engineers and the American Institute of Aeronautics and Astronautics. He retired from the U.S. Air Force as a Lieutenant Colonel, and is now a gentleman engineer, consultant, technical writer, editor, and novelist.

# Contents

# 1 Main Features of UWB Radars and Differences from Common Narrowband Radars

*Igor I. Immoreev*

## CONTENTS



## 1.1 INTRODUCTION

The majority of traditional radio systems use a narrow band of signal frequencies modulating a sinusoidal carrier signal. The reason is simple: a sine wave is the oscillation of an LC circuit, which is the most elementary and most widespread oscillatory system. The resonant properties of this system allow an easy frequency selection of necessary signals. Therefore, frequency selection is the basic way of information channel division in radio engineering, and the majority of radio systems have a band of frequencies that is much lower than their carrier signal. The theory and practice of modern radio engineering are based on this feature.

Narrowband signals limit the information capability of radio systems, because the amount of the information transmitted in a unit of time is proportional to this band. Increasing the system's information capacity requires expanding its band of frequencies. The only alternative is to increase the information transmitting time.

This information problem is especially important for radiolocation systems, where the surveillance time of the target is limited. Past radars have used a band of frequencies that does not exceed 10 percent of the carrier frequency. Therefore, they have practically exhausted the information opportunities in terms of range resolution and target characteristics. A new radar development is the transition to signals with a wide and ultra-wide bandwidths (UWBs).

For designing UWB radars, as with any other equipment, we must understand the required theory that will allow us to correctly design and specify their characteristics. The theory is also necessary for defining the requirements of radars and for developing the equipment needed to create, radiate, receive, and process UWB signals. In spite of recent developments and experimental work, there is no satisfactory and systematized theory of UWB radars available. The reason is that the process of radar-tracking and surveillance with UWB signals differs considerably from similar processes when using traditional narrowband signals. The study of these differences helps us to

0-8493-4267-8/01/$0.00+$.50

understand when the traditional theory of radar-tracking detection can and cannot be used for designing UWB radars. When traditional theory cannot be used, then we must develop new methods.

In this chapter, we will examine the new information opportunities that result from applying UWB signals in radars, and the basic differences between UWB radars and narrowband radar systems.

## 1.2 INFORMATION POSSIBILITIES OF UWB RADARS

The informational content of the UWB radars increases because of the smaller pulse volume of the signal. For example, when the length of a sounding pulse changes from 1 μs to 1 ns, the depth of the pulse volume decreases from 300 m to 30 cm. We can say that the radar instrument probing the surveillance space becomes finer and more sensitive.

The UWB radar's reduced signal length can

1. Improve detected target range measurement accuracy. This results in the improvement of the radar resolution for all coordinates, since the resolution of targets by one coordinate does not require their resolution by other coordinates.
2. Identify target classes and types, because the received signal carries the information not only about the target as a whole but also about its separate elements.
3. Reduce the radar effects of passive interference from rain, mist, aerosols, metallized strips, etc. This is because the scattering cross section of interference source within a small pulse volume is reduced relative to the target scattering cross section.
4. Improve stability when observing targets at low elevation angles at the expense of eliminating the interference gaps in the antenna pattern. This is because the main signal, and any ground return signal, arrive at the antenna at different times, which thus enables their selection.
5. Increase the probability of target detection and improved stability observing a target at the expense of elimination of the lobe structure of the secondary-radiation pattern of irradiated targets, since oscillations reflected from the individual parts of the target do not interfere and cancel, which provides a more uniform radar cross section.
6. Provide a narrow antenna pattern by changing the radiated signal characteristics.
7. Improve the radar's immunity to external narrowband electromagnetic radiation effects and noise.
8. Decrease the radar "dead zone."
9. Increase the radar's secretiveness by using a signal that will be hard to detect.

## 1.3 HOW UWB RADAR DIFFERS FROM CONVENTIONAL RADAR

### 1.3.1 Signal Waveform Changes during Detection and Ranging Processes

Narrowband signals (i.e., sinusoidal and quasi-sinusoidal signals) have the unique property of keeping their sinusoidal shape during forms of signal conversions such as addition, subtraction, differentiation and integration. The waveforms of sinusoidal and quasi-sinusoidal signals keep a shape identical to that of the original function and may differ only in their amplitude and time shift, or phase. Hereinafter, *shape* is understood as the law of change of a signal in time. On the contrary, the ultra-wideband signal has a nonsinusoidal waveform that can change shape while processing the above specified and other transformations.

Let us assume that a UWB signal $S_1$ shown in Figure 1.1 is generated and transmitted to the antenna in a form of a current pulse. The first change of the UWB signal shape $S_2$ occurs during

pulse radiation, since the intensity of radiated electromagnetic field varies proportionally with the derivative of the antenna current.

The second change of the shape occurs when pulse duration in the space $c\tau$ (where $c$ is velocity of light, $\tau$ is the pulse duration in the time domain) is less than linear size of the radiator $l$. When current changes move along the radiator, then electromagnetic pulses are emitted from radiator discontinuities. As a result, a single pulse transforms into a sequence of $k$ pulses divided by time intervals $\tau_1, \tau_2, \ldots, \tau_{k-1}$, shown as $S_3$ in Figure 1.1. The apparent radiator length changes according to variations of the angle $\theta$ between the normal to the antenna array and the direction of the wave front. Therefore, interpulse intervals vary with this angle as follows:

$$\tau_1 \cos\theta, \quad \tau_2 \cos\theta, \ldots, \tau_{k-1} \cos\theta$$

The third change of the shape occurs when the signal is radiated by a multi-element antenna array composed of $N$ radiators with a distance $d$ between them. The pulse radiated by one antenna element at the angle $\theta$ is delayed by the time $(d/c)$ sin $\theta$ compared to the pulse radiated by the adjacent antenna element. The combined pulse will have various shapes and duration at different angles $\theta$ in the far field as equation $S_4$ in Figure 1.1. Far-field pulse shapes at different angles $\theta$ are shown in Figure 1.2. Note that the combination of multiple square pulses radiated by the four-element antenna array and shifted in time over different angles have waveforms very different from the radiated rectangular video pulse.

The fourth waveform change is $S_5$ in Figure 1.1, and it occurs when the target scatters the signal. In this case, the target consists of $M$ local scattering elements, or bright points, located along the line $L$. If the UWB signal length is $c\tau << L$, then the each discrete target element reflects the

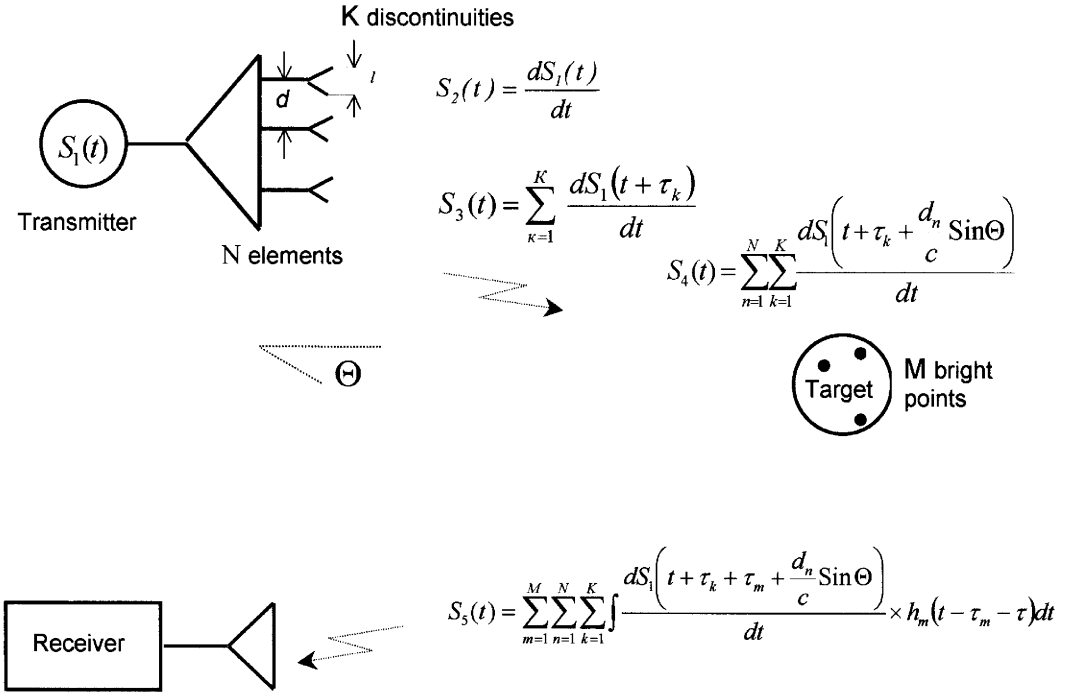


**FIGURE 1.1** Radar signal waveform changes during transmission, target reflection, and reception. UWB waveforms may change radically during the target detection process.

signal and forms a pulse sequence of $M$ pulses. The actual number of pulses, time delay $\tau_m$, and intensity depend on target shape and target element pulse response $h_m$. This pulse sequence is called the *target image.* The whole image represents the time distribution of scattered energy that was formed during time interval $t_o = 2L/c$.

So, for the high-resolution UWB target case, the radar cross section (RCS) becomes time-dependent, and now we must introduce the concept of an instantaneous target RCS. The image will change with viewing angle variations. In this case, the target secondary pattern is nonstationary and variable. Because target scattered signals will form no secondary pattern "nulls," this promotes steady target viewing.

Some target elements may have a frequency bandwidth that is out of the UWB signal spectrum, so these will act as frequency filters and change the shape even more. Note that, in this case, the radar return signal not only indicates the presence of the target but carries back much information regarding the target. If the target were smaller than the radar pulse length $c\tau$, then no such information would be available.

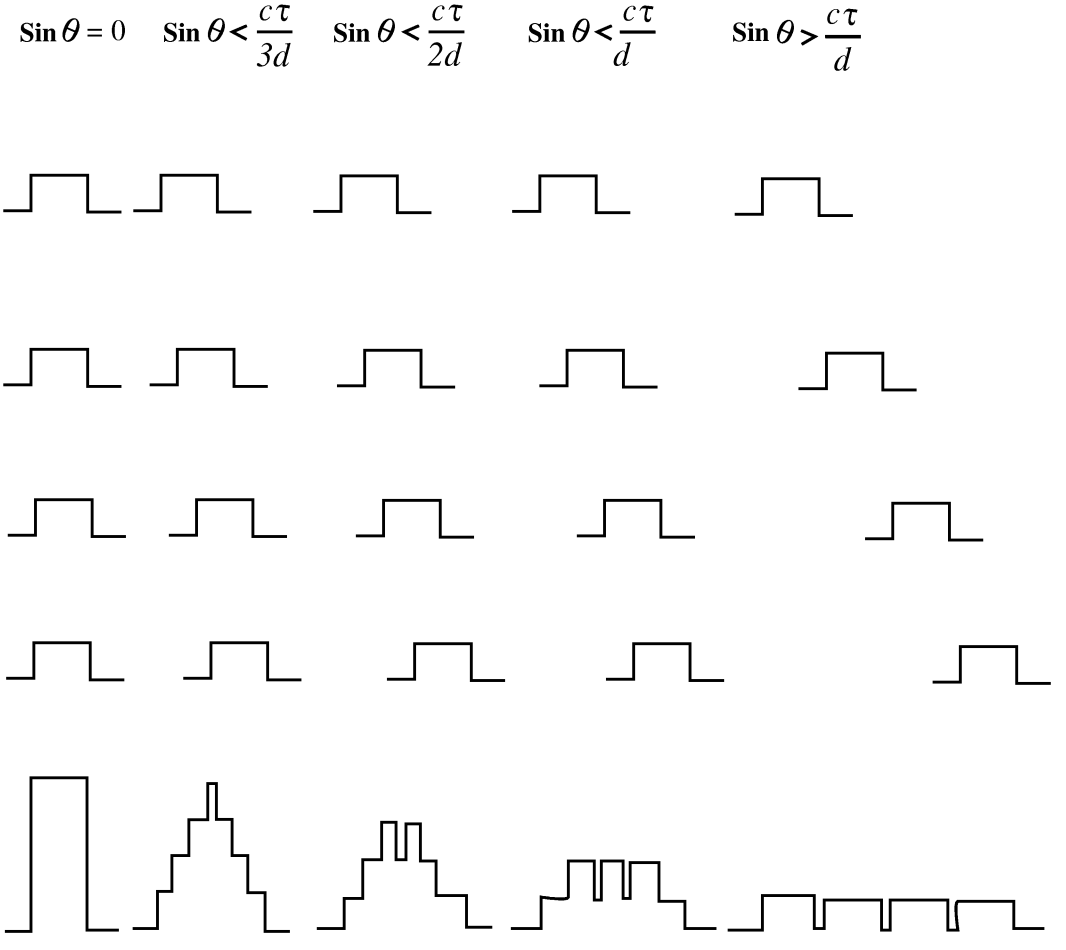


**FIGURE 1.2** If a four-element array antenna shown in Figure 1.1 transmits UWB rectangular pulses, their far-field shapes will vary with the off-axis angle θ.

The fifth change occurs during signal propagation through the atmosphere because of different signal attenuation in various frequency bands.

The sixth change of the shape occurs during signal reception. The reason for this is the same as for radiation, i.e., the time shift between current pulses induced by the electromagnetic field in the antenna elements located at various distances to the target. Figure 1.3 shows an example of an actual UWB signal reflected from a target with multiple scattering centers.

Following this discussion, we conclude that the UWB signal shape changes many times during radar viewing. It is difficult to describe such signals analytically. Conventional optimal processing using matched filters or correlators is unsuitable for these signals because of the changing waveform. Therefore, one of the most important problems with UWB radar is the development of signal processing methods that maximize signal-to-noise ratio when we perform the detection of the UWB signals.

### 1.3.2 How the UWB Signal Waveform and the Antenna Characteristics Mutually Affect Each Other

In Figure 1.2, we can see as the waveform of the UWB signal changes depending on the off-axis angle. For the example of a rectangular pulse, the off-axis signals have the same energy but are changed in waveform to have a longer duration and less peak power. It is quickly apparent that our traditional concept of a single-frequency antenna directional pattern (DP) of the field no longer applies to UWB signals. The antenna directional pattern for UWB signals is measured for either peak or average power. This DP is formed only during radiation, which means that a UWB pattern is an instantaneous antenna pattern.

Let us consider DP for the peak power $P(\theta, \phi)$ for the $N$ radiating element antenna array. For an example, we will take one main cross section of this DP, $P(\theta)$. Let us assume that the field video

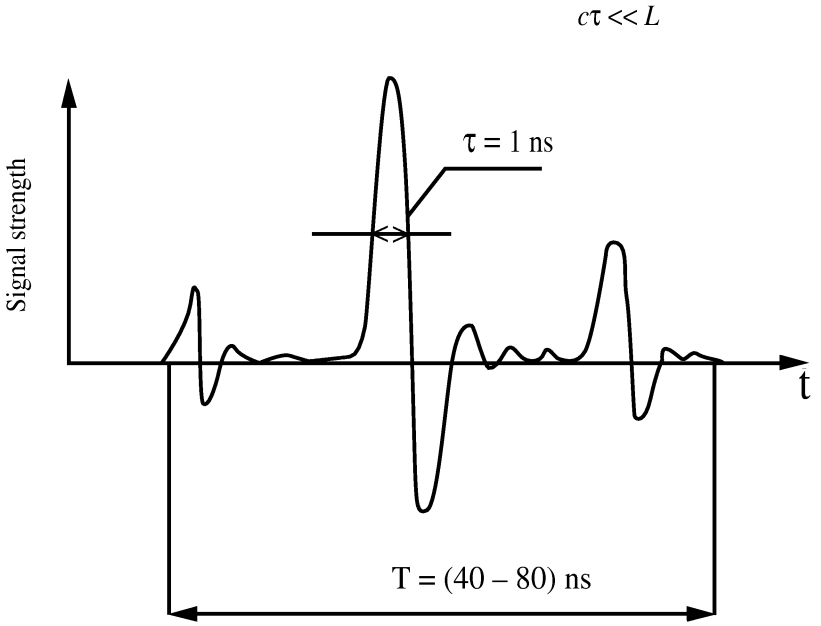


**FIGURE 1.3** An example of a high-resolution UWB signal return from a target with three distinct scatterers.

pulse radiated by a single radiator of the array has a rectangular waveform, the duration $\tau$, and a peak power $P_1$. It is clear that the video pulses going from all radiators along the normal will arrive simultaneously at a receiving point. The peak power value at this point is $P_{max} = NP_1$.

As the angle $\theta$ increases, the time delay between video pulses is increasing. At an angle $\theta_1$, when $sin\ \theta_1 = c\tau/(N-1)d$, the peak power falls by jump in size $P_1 = (1/N)\ P_{max}$ and becomes equal to $(1 - 1/N)P_{max}$. When $sin\ \theta = sin\theta_2 = c\tau(N-2)d$, then the peak power falls once more for $(1/N)P_{max}$ and becomes equal to $(1 - 2/N)P_{max}$. So long as there is some angle $\theta_{N-1}$, then the level of peak power will achieve the minimal value $(1/N)P_{max} = P_1$, which will be the background DP level. Thus, at the rectangular form of a radiating pulse DP, there is a step function as follows:

$$P(\theta) = \sum_{m=-(N-1)}^{m=N-1} (N-m)P_1 \times \delta(\theta - \theta_m)$$

where $\delta(\theta)$ for a single pulse is $\delta(\theta - \theta) = \begin{cases} 1 \text{ if } \theta = \theta_m \\ 0 \text{ if } \theta \neq \theta_m \end{cases}$

The formulas relating the angle $\theta$ and quantity $\tau$ and $d$ at various values of peak power are given for $N = 4$ in Figure 1.2. Now, Figure 1.4 shows how the DP $P(\theta)$ for same array varies with different values of $\theta$. DP are represented for three quantities of the angle $\theta_1$, that is for three variants of the ratio $\tau$ and $d$. From the expressions presented, it is clear that the values of angles $\theta_1$, $\theta_2$, . . . , and, consequently, the DP width and the gain factor of an antenna can be changed by varying the radiator spacing $d$ and the video pulse duration $\tau$, and the pulse waveform in the general case. Figure 1.4 also is shows the DP for a case where $c\tau << d$ so that $\theta$ is nearly zero degrees. In this case the main lobe is so compressed that it is approaching a line and the side radiation continues to be a background of $(1/N)^2$ level.

These DP $P(\theta)$ is actually a multiplier of the array. To get the antennas complete DP, we must also consider the single radiator's directional pattern.

Figure 1.5 shows the DP of an array made of a great number of radiators ($N > 100$) and radiating different pulse durations. The diagrams are normalized on the maximum level. Notice that the beamwidth depends on duration of pulse, and the side radiation of an array presents a uniform background and does not have the characteristic large side lobes of narrowband antennas.

Earlier, we considered the case of an antenna radiating a single pulse. If the antenna array radiates a sequence of pulses under an angle $\theta_0$, as shown on Figure 1.6, there is a second maximum DP, similar to an interference beam DP by the narrowband antenna array. It occurs due to addition of pulses radiated in the next periods of recurrence. However, for a narrowband array, the interference beam arises at shift of the next radiators waveform for the period of the high frequency. In a UWB array, the similar second maximum arises at the shift of pulses from the next radiators for the period of recurrence, which considerably exceeds the period of high frequency. It allows us to choose the pulse repetition frequency and UWB array spacing that is rather large, and by that to reduce total of its channels.

The DP presented on the figures corresponds to the rectangular waveform of the field video pulse in the space, and so the DP shape for peak and average powers will be different for the other waveform of the field video pulse. Thus, the antenna DP for the UWB signal depends not only on angular coordinates but also on the time-dependent waveform, which is designated $S$. Therefore, the expressions for the UWB signal DP will take the form $P(\theta, \phi, S, t)$ and $W(\theta, \phi, S, t)$. The signal waveform $S$ relates to its spectrum $F$ by the Fourier transform. Therefore, the expressions for DP can be written in the form: $P(\theta, \phi, F, \omega)$ and $W(\theta, \phi, F, \omega)$. However, the basic features of the UWB signal DP indicated above for the rectangular video pulse of a field are retained for other waveforms or signal spectra.

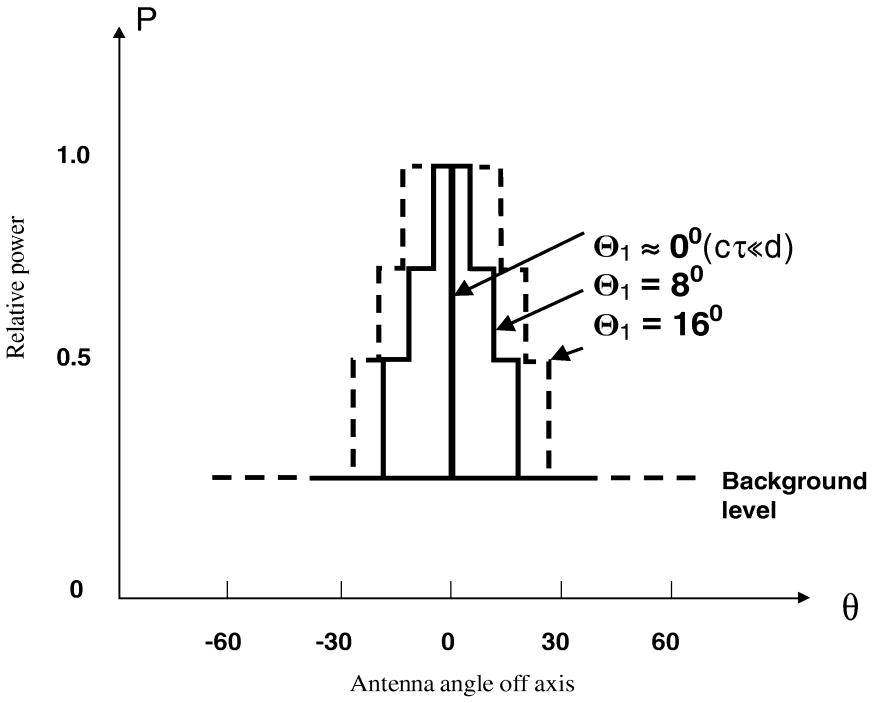


**FIGURE 1.4** The directivity pattern $P(\theta)$ for a four-element antenna array with rectangular UWB pulse waveform.

Since the DP of an antenna radiating or receiving the UWB signal becomes dependent on the signal waveform and duration, then it is obvious that the directivity factor $G(\theta, \phi, S, t)$, then the gain factor $K(\theta, \phi, S, t)$ of an antenna and its effective cross section $A(\theta, \phi, S, t)$ become also dependent on the signal parameters. As a result, the directivity factor for the UWB signal is the ratio of the density of the UWB signal power radiated by an antenna in a specified angular direction in the UWB signal bandwidth to the density of the same power signal from an uniformly isotropic radiator in the same bandwidth.

In the case of such determination, the directivity factor depends not only on the geometry of an antenna but also on matching the signal spectrum to the frequency response of an antenna. As a result, the calculation of the antenna directivity factor for the UWB signal presents great difficulties and, for the moment, it can be performed only for its simplest forms.

The main conclusions are as follows:

1. The antenna DP for the UWB signal is a space-time (space-frequency) function, the characteristics of which depend both on the geometry of an antenna and the signal parameters.
2. The width and shape of the DP of the array of radiators for the UWB signal are determined by the waveform and duration of a video pulse radiated, on the one hand, and the size of aperture and the radiator spacing, on the other hand, and also by the shape of the DP array radiator.
3. Interference effects inherent in narrowband signals are not present when the UWB signal is radiated. This circumstance leads to the lack of lobes in the DP structure. In this case, the increase in the distance between array elements allows for making the DP extremely narrow without the appearance of additional diffraction maxima.

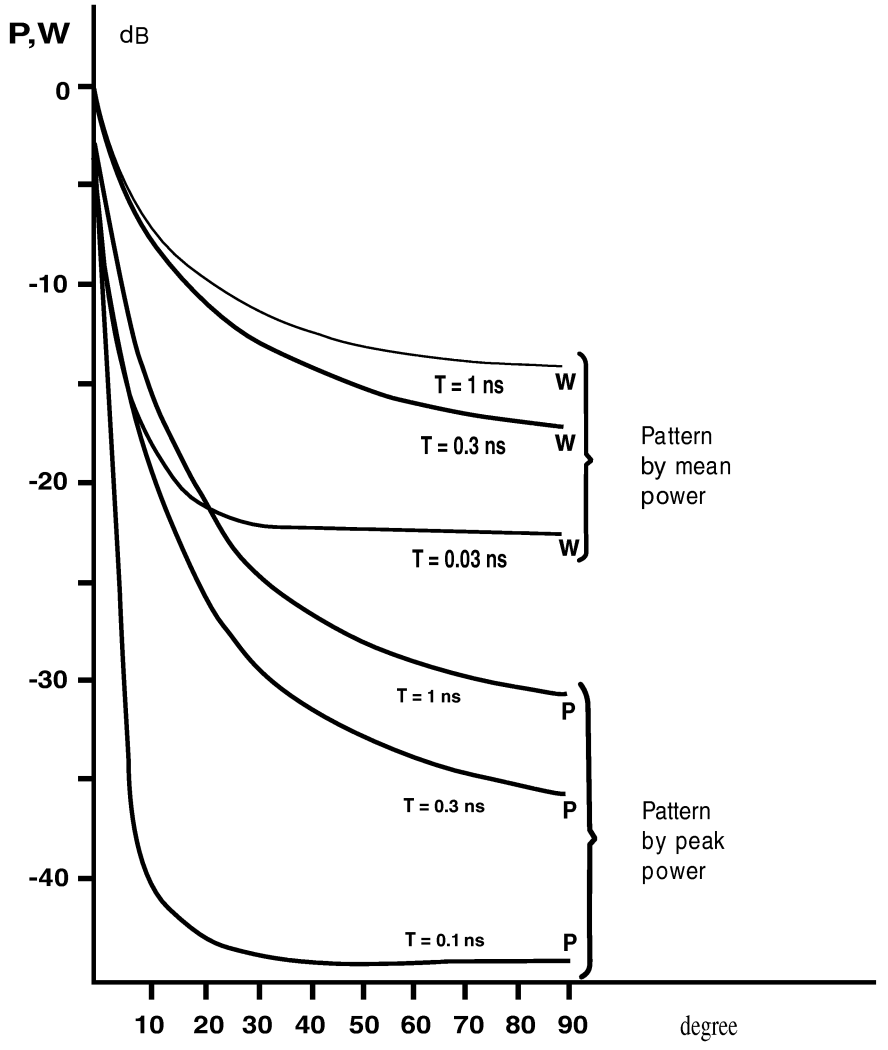


**FIGURE 1.5** Peak and average power directivity patterns for a multi-element array with more than 100 radiators and different UWB video pulse lengths. The sharp beam forming for shorter-duration signals results from the waveform distortion off axis, as shown in Figure 1.2.

4. The directivity factor and the effective cross section of antennas using UWB signals are functions of time and the shape of the signal.

### 1.3.3 The Target Scattering Cross Section for UWB Signals

One of the most complicated matters in the UWB location is the problem of signal reflection from targets and the target scattering cross section obtained when using these signals. The formal calculation of the scattering cross section, which does not depend on the signal waveform, is given by

$$\sigma = 4\pi R^2 \frac{E_s^2}{E_0^2}$$

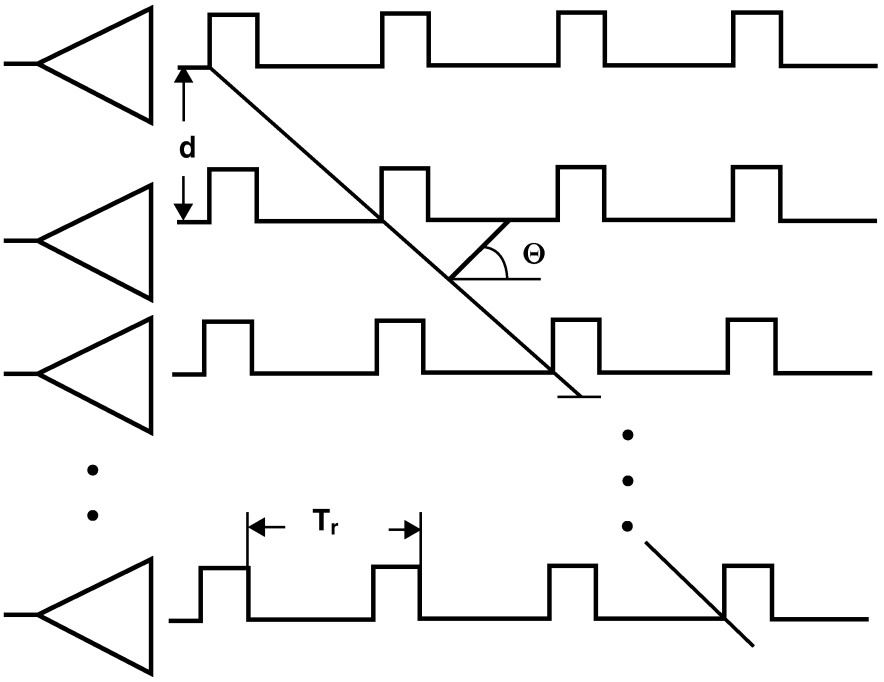


**FIGURE 1.6** A linear array antenna can form a secondary maximum due to the addition of sequentially radiated pulses. This consideration will be important for designing array antennas for coded pulse sequence signals, which could form significant second maximum sidelobes. This is another example of UWB antenna patterns being dependent on signal format.

where $R$ is the distance to a target for which a wave incident on it can be considered as a plane one; $E_S$ is the intensity of the electric field, which is determined by the target reflection, at the radar receiving antenna; and $E_0$ is the intensity of the electric field incident on a target. In essence, this formula compares the power density of a reflected wave arriving at the radar with the power density of a target-incident wave.

Scattering theory generally assumes that the individual elements of a target scatter the energy of an incident wave independently of one another, so this target is considered as a total set of elements, each of them being an independent brilliant point. Generally speaking, such a representation of a target is not sufficiently justified, since the target elements can be mutually shadowed, and also multiple reflections of a wave are possible between the elements of a target.

Let us consider the process of signal reflection from an individual brilliant point. The parameters of a reflected pulse will depend on the waveform of the pulse response characteristic of a local element and can be determined as the convolution of this characteristic, $h(t)$, with the function $f(t)$ describing a target-incident signal. The integral transformation of the frequency response of a signal-spectrum target can be used for this purpose.

The pulse response characteristic of a local element, $h(t)$, can be derived in the general form by solving the Maxwell equations for a signal defined as the delta-function $\delta(t)$ or its approximation and the space area that does not contain irrelevant current sources. However, the solution of these equations in the general form can be made only for a limited number of simplest elements and cannot find wide application.

The geometrical optics techniques are relatively simple, but they do not provide an answer in a number of cases and, in particular, for plane surfaces. The physical optics techniques allow for solving this problem, but they do not provide the answer at the shadow boundary. The physical

and geometrical theories of diffraction enable us to correct results obtained within the approximation of the physical and geometrical optics, but they do not allow for estimating the contribution of a surface traveling wave to the signal scattering over an arbitrary-shape body. The matter is that a significant contribution to the pulse response characteristic of various targets is made by the so-called *creeping waves,* which are the surface waves propagating in the shadow region and enveloping a scatterer. A whole number of new techniques has been recently developed for their account, the singular expansion technique being the most efficient of them. However, it should be stated that the theoretical and computational means are not currently available to offer a reasonably accurate estimate of the scattering cross section of a complex target irradiated by the UWB signal.

Let us consider the difference between reflected signals when a target is irradiated by narrowband and UWB signals. The spatial physical length of a narrowband signal is equal to $c\tau_{NB} \geq L$, where $L$ is the size of a target and $c\tau_{UWB} \leq L$ for an UWB signal. The "long" narrowband signal reflected from all $N$ brilliant points will present a sum of $N$ arbitrary-phase harmonic oscillations or their vector sum. In this case, the target scattering cross section is equal to

$$\sigma_{NB} = \sum_{k=1}^{N} \sigma_k \cos\left(2\pi \frac{R}{\lambda}\right)$$

where $\sigma_k$ = the scattering cross section of a brilliant point number $k$
$R$ = the distance from the radar to this point

Since a sum of one-frequency harmonic oscillations is also a harmonic oscillation, then the reflected signal will present an invariable amplitude and arbitrary-phase sinusoidal wave.

The summation of harmonic signals reflected from the different points of a target may lead, in respect to some angular directions, to the compete compensation of the field reflected in the radar direction, which is equivalent to the null formation in the secondary target DP.

We have a different picture when the UWB signal, which has $c\tau_{UWB} << L$, is reflected from a target. In this case, the reflected signal will represent the sequence of $N$ video pulses randomly arranged in the interval and $T = L/c$, forming the so-called image of a target, as shown in Figure 1.3.

Video pulses making the whole image may have different amplitude. It depends on the scattering cross section of the corresponding brilliant point of the target. The polarity of these pulses may change. This depends on the magnetic permeability of the material that reflects the signal. When reflecting from a conductor, the electric component of the field changes its polarity. However, when reflecting from materials with high magnetic permeability, the wave polarity does not change. Finally, video pulses reflected from the target may change their initial (e.g., rectangular) form. This will happen if the brilliant points of the target have resonance properties as well as the frequency range that is less than the spectrum of the UWB signal. Besides, the form of the reflected signal will be complicated by re-reflections of video pulses from the brilliant points.

As a result, the target scattering cross-section becomes time-dependent so that $\sigma_{UWB} = \sigma_{UWB}(t)$. If the UWB signal processing algorithm allows for adding the reflections from individual brilliant point (see Chapter 2 of this book), then the target scattering cross section is not time dependent.

$$\sigma_{UWB} = \sum_{k=1}^{n} \sigma_k$$

If we assume that each brilliant point of a target reflects equal energy, then $\sigma_{UWB} \geq \sigma_{NB}$ actually in all cases, since

$$\left| \sum_{k=1}^{n} a_k \cos\phi \right| \leq \sum_{k=1}^{n} \alpha_k$$

Thus, the UWB signal provides a gain in the scattering cross section magnitude. This circumstance, as well as the absence of nulls in the secondary DP of a target, favors a more stable target observation.

- Two factors determine the UWB signal conversion when it is scattered by a target. The first one is related to the geometry and orientation of a target and leads to the conversion of one radiation video pulse into a video pulse burst. The second factor is related to the difference of the waveform (or spectrum) of a signal irradiating the target element from the pulse response (or frequency) characteristic of this element. This circumstance results in the change of the waveform of a single video pulse of the burst.
- For the UWB signal, the target scattering cross section is a time function. In the case of the matched processing of the reflected UWB signal, the target scattering cross section will be larger than that for a narrowband signal. The secondary DP of a target will not have nulls arising under the action of a narrowband signal owing to the interference of waves reflected from different target elements. This circumstance provides for a more reliable and stable reception of reflected signals.

### 1.3.4 The UWB Radar Range Equation

The important aspect of the theory of radar observation when using UWB signals is the change in the meaning of parameters in the range equation. In the case under consideration, the directivity factor of a transmitting antenna, $G$, the effective cross section of a receiving antenna, $A$, and the effective scattering cross section of a target, $\sigma_{UWB}$, become dependent on time and signal parameters; i.e., they are nonstationary. Now, this equation involves not only constants but time functions. This feature leads to the other form of the range equation wherein the range is a nonstationary quantity and varies depending on the signal waveform and time.

$$R(s,t) \le \sqrt[4]{\frac{EG(\theta,\phi,S,t)\sigma_{UWB}(t)A(\theta,\phi,S,t)}{(4\pi)^2 \rho q N_0}}$$

where $E$ = the energy of a radiated signal
$\rho$ = the losses in all the systems of a radar
$q$ = the threshold signal-to-noise ratio
$N_0$ = the spectral density of noise power

It should be noted that a UWB radar features specific energy losses that are not found in narrowband radars. For instance, under the conditions of short-pulse transmission, losses arise owing to the antenna rejection of the lower frequencies of the signal spectrum and the mismatch of this signal to the frequency response of an antenna. Calculation of the magnitude of losses and ways to allay these losses are considered at the end of this chapter.

Under such conditions, these losses may be caused by the absence of information on the space parameters of targets. Losses can reach 10 to 12 dB in the case of the mismatched processing of a signal reflected from a target when the dimensions of this target and the number of its brilliant points are not known. The distinctive features of UWB signals processing are considered in Chapter 2 of this book. The same section contains description of the suggested method to process such signals and avoid the above mentioned losses.

### 1.3.5 Electromagnetic Compatibility

When UWB radars are used, an important problem is presented by their electromagnetic compatibility with other radio electronic systems and facilities because, in this case, the frequency diversity of other systems is practically impossible.

When UWB radar operates jointly with conventional narrowband radar, only a slight portion of the UWB radar signal energy enters the frequency bandwidth of the narrowband radar receiver. Really, the time constant of the input circuit of a narrowband receiving device, $\tau_1 = 1/\Delta f$, which determines the rise time of the input signal amplitude up to the prescribed value, will be much longer than the pulse length of an UWB radar, $\tau$. The bandwidth of a given UWB radar and that of the narrowband radar may differ by three orders of magnitude pulse lengths, e.g., 1 ns and 1 μs. This means that jamming occurring in the narrowband radar receiver due to this UWB pulse of duration $\tau$ has no time to reach a noticeable magnitude in the receiver.

Besides, when both narrowband radar and UWB radar radiate equal powers, this UWB radar has the unit power per unit of the bandwidth (W/MHz), which is approximately lower by three orders of magnitude. This means that only about one-thousandth of the UWB signal power arrives at the narrowband radar receiver. As a result, the total attenuation of the UWB signal in the narrowband radar receiver is about 60 dB, as compared with the influence of the signal of similar narrowband radar on this receiver. An additional effect may be provided if narrowband radars use asynchronous jamming protection equipment and the range selection of received signals. Figure 1.7 shows the dependence of the attenuation factor of the UWB radar interference, $k$, on the carrier frequency, $f$, of narrowband radar where, in the figure, $\Delta f$ *is* the narrowband system bandwidth and $F$ is the UWB radar signal bandwidth.

When a narrowband radars interferes with a UWB radar, one efficient jamming protection is the frequency rejection by cutting narrowband radar signals out the UWB radar signal spectrum. This is usually done during signal processing, as shown in several of the experimental radar sets in Chapter 12.

When two or more UWB radars operate jointly, it is advisable to use the time division of the signals of stations. Because of the short UWB radar signal length and the relative pulse duration reaching value of $10^6$ to $10^7$, the interference of neighboring radar occupies a very small range

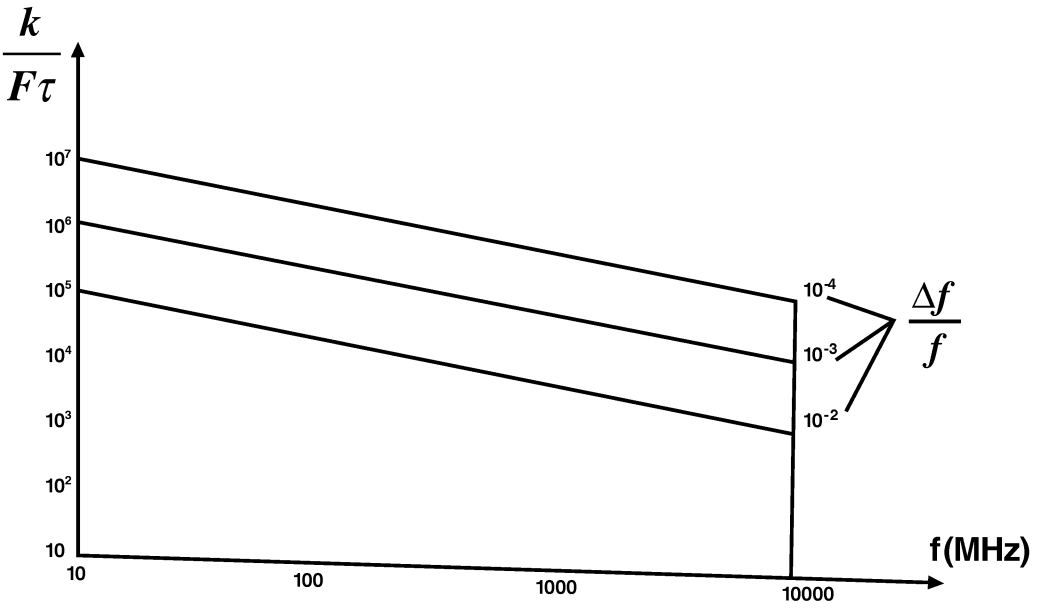


**FIGURE 1.7** A narrowband radar will have a long time constant defined by the center frequency and bandwidth. Short UWB radar signals will be attenuated, because they are much shorter than the narrowband system time constants.

section. When radars are mutually synchronized, this section can be blanked without adverse effects to target detection. Interference gating is possible in the radar computer after the estimation of the coordinates of an interfering station has been performed. Considering that interference owing to its short length occupies an insignificant portion of the range, its presence featuring corresponding coloration may be allowed in the output data of a station. The computation show that the area of the mutual influence of UWB radars does not exceed 70 to 80 km at 1 MW peak radiated power. On the other extreme, interference from narrowband systems is a major problem in UWB radar design.

## 1.4 MOVING TARGET SELECTION IN THE UWB RADAR AND PASSIVE JAMMING PROTECTION

The detection of airborne targets by ultra-wideband (UWB) radar involves interference problems from both natural and man-made sources. The selection of a moving target detection system must be designed around the particular UWB radar system technical features. On the one hand, considerable reduction of the pulse volume substantially decreases the target scattering cross section of the interference, facilitating the observation of the target on its background. On the other extreme, the small pulse volume enhances the influence of those interference elements that can change their position by entering or leaving the pulse volume for the pulse-repetition period. These sources increase the uncompensated residues at the output of the interleaved periodic compensation (IPC) system, thus reducing its effectiveness. The present section is devoted to the investigation of these peculiar features and their influence on the interference immunity of the UWB radar provided with the IPC.

A small pulse volume permits moving targets to be separated without using the Doppler effect. If, over the repetition period $T_r$, a target travels a distance exceeding a range element (30 cm at $\tau = 1$ ns), then, when interleaved periodic subtraction is applied, the signal of this target will be separated, and the signals of stationary or low-mobility targets will be suppressed. Such and IPC system must the following condition to operate:

$$\frac{c\tau}{2} \leq v_R T_r$$

where $v_R$ = the radial velocity of a target

This system of selection lacks "blind" velocities and does not impose special requirements on the coherence of radiated signals. The target velocity is always unambiguously measured. The target radial velocity $v_R$ can be determined in the selection system by the variation of the range to a target. The minimum determined velocity of a target would be equal to

$$v_{R\,\min} = \frac{c\tau}{2T_r}$$

One of the main characteristics of the passive interference that determines the effectiveness of the moving target selection (MTS) system is the correlation function of the interfering reflections. Let us consider its peculiar features with respect to the UWB signal.

Figure 1.8 gives the normalized correlation functions of the passive jamming $R_n$ at different values of $\tau$. As shown in the figure, for the narrowband signals, the correlation function depends very little on the pulse duration. However, at $\tau < T_{av}$ (where $T_{av}$ = the period of oscillation at the average spectrum frequency, and $\sigma_d$ = the root-mean-square deviation of the Doppler frequency of the interference), then the decorrelation of the passive interference is observed as the pulse duration

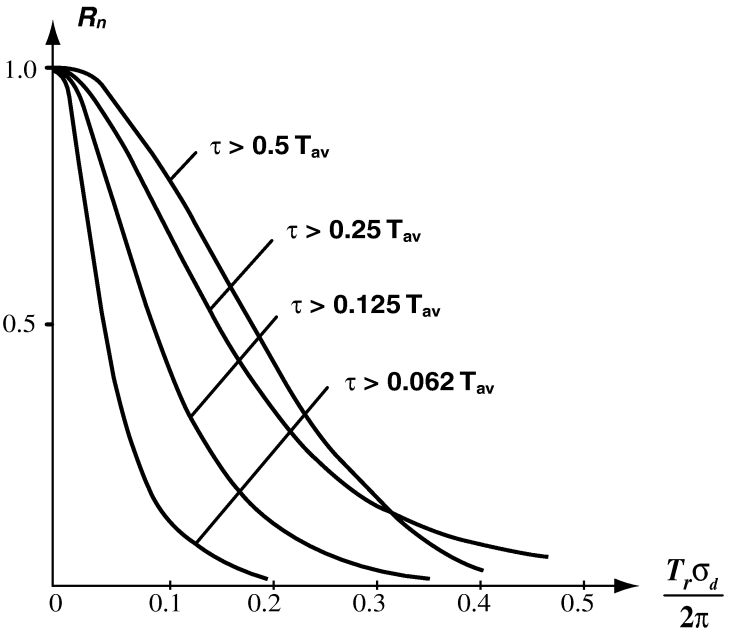


**FIGURE 1.8** Moving target Doppler signals will cause passive interference or jamming. This plot shows the normalized correlation functions of passive jamming for different values of signal lengths.

is decreased. Physically, it can be explained by the fact that the decrease of the duration of pulse $\tau$ brings about the increase of the maximum and, consequently, medium frequency of the spectrum. As a result, the spectrum of the moving passive interference is extended, which reduces the effectiveness of the MTS. On the other hand, with the reduction of the pulse duration, the pulse volume is decreased and, respectively, the power of the passive interference is diminished. Therefore, the interference immunity of the UWB radar should be considered taking account of two opposite factors for a decrease in the pulse duration.

1. The reduction of the pulse volume (i.e., decrease in the power of the passive interference)
2. An increase in the interperiodic decorrelation of the passive interference (i.e., the decrease in the coefficient of suppression of the MTS)

Figure 1.9 shows the dependence the signal-to-interference ratio $Q$ at the output of the systems of the single and twice interleaved periodic compensation (IPC-1 and IPC-2) on duration of UWB signal $\tau_t$ at different values of period repetition $T_r$. The value $Q$ is normalized rather so that $Q_0$ is the signal-to-interference ratio at $\tau_t = T_{av}$ and at relative width of a spectrum of passive interference $\sigma_d T_r/2\pi = 0.1$. As it follows from the figure, there are two extremes. The first of them (maximum) falls on the values of duration of the pulse $\tau_t = 0.5T_{av}$. At $\tau_t > 0.5T_{av}$ prevailing is the first factor, and at $\tau_t < 0.5T_{av}$ is the second. With the further decrease in $\tau_T$, the MTS stops influencing the interference immunity because of complete decorrelation of the interference, and only the first factor remains—reduction of the pulse volume. The level of interference is once again decreased, and $Q$ increases. Thus, the position of the second extreme (minimum) corresponds to the complete decorrelation of the interference and absence of the velocity selection. For the most effective rejecter (IPC-2), these regularities are displayed more distinctly due to the stronger sensitivity to the correlation properties of the interference.

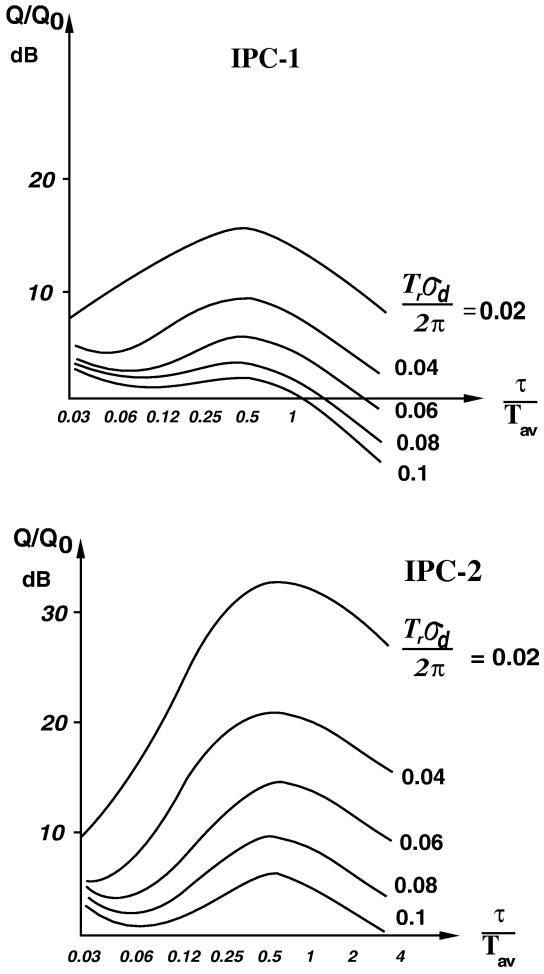


**FIGURE 1.9** Moving target selection depends on the pulse length and the effects of signal-to-interference ratios at the system output; shown here for single (IPC-1) and double (IPC-2) interleaved periodic compensation for $\tau = T_{av}$ and $\sigma_d T_r/2\pi = 0.1$.

Let us note that, with the decrease in the relative width of the passive interferences spectrum, $\sigma_d T_r/2\pi$, the position of the second extreme is shifted to the left toward the lower-duration $\tau$. It means that, with the decrease in the width of the Doppler spectrum of the interference and increase in the pulse repetition frequency, the complete decorrelation of the interference will occur with the shorter signal duration. Within the limits for the non-fluctuating passive interference the decrease in the pulse duration does not influence the MTS effectiveness. Thus, using MTS with respect to the UWB signal is advisable with rather narrowband interferences (local objects) in the radar with the relatively high repetition frequency (i.e., with the small range).

## 1.5 SHORT VIDEO PULSE FEATURES IN UWB RADAR

One of the peculiar features of the UWB radar operating with short video pulses with duration $\tau$ is additional losses of energy. The point is that any antenna does not radiate in the range of frequencies lower than some $f_{min}$. On the other hand, the frequency spectrum of any video pulse

has the maximum at the zero frequency. The basic energy of the pulse is concentrated in the band of frequencies $\Delta f$ and restricted by some $f_{max}$ usually lying in the region of the first zero of its spectrum. As a result, the frequency characteristic of the antenna and spectrum of the signal appear to be unmatched. Part of the energy that did not fall into the antenna frequency band will be lost. This is seen well in Figure 1.10, which gives the frequency characteristic of the Hertzian dipole $P$ (length $l$) and spectrum of the rectangular pulse $S$. With respect to the signal, the antenna is essentially a high-frequency filter.

The notion of the spectral efficiency $\eta_{\Delta f}$ was introduced to account for these losses and is a part of the total efficiency of the transmitting device. This efficiency determines the relative share of the energy of the sounding pulse falling into the operating frequency band of the antenna.

$$\eta_{\Delta f} = \frac{W_{\Delta f}}{W_s}$$

where $W_S$ = full pulse energy

$W_f$ = the energy of that part of the pulse spectrum falling into the antenna frequency band

For the single-polarity pulses, the spectral losses can be rather significant. It is possible to reduce these losses by selecting an optimal duration, $\tau_{opt}$, for each pulse form in the given band of frequencies that will have the maximum value $\eta_{\Delta fopt}$ spectral efficiency. The curve "a" in Figure 1.11 shows the dependence of $\eta_{\Delta fopt}$ on $\Delta f$ for three simple single-polarity pulses: rectangular, bell-shaped, and triangular. For all considered pulses at $\Delta f < 3$, the maximum efficiency $\eta_{\Delta f\, max} < 50\%$, which essentially worsens the efficiency of a radar.

The spectral efficiency $\eta_{\Delta f}$ can be improved by changing the radiating pulse spectrum. With this aim in mind, spectrum $S_2(f)$ of the correcting pulse $u_2(t)$ is subtracted from spectrum $S_1(f)$ of the basic single-polarity pulse $u_1(t)$. The form and intensity of this spectrum were selected so that,

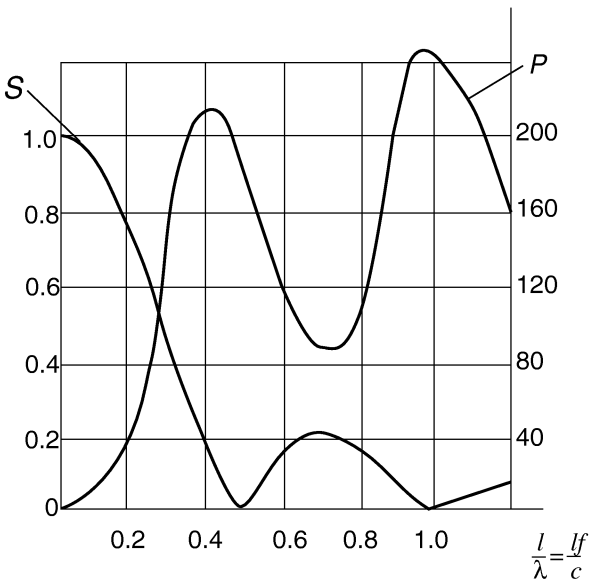


**FIGURE 1.10** Antennas are a major cause of energy loss in transmitting UWB signals. This shows the frequency response of a dipole antenna $P$ and the spectrum of a video pulse $S$. The antenna will distort the signal by passing only the higher-frequency components.

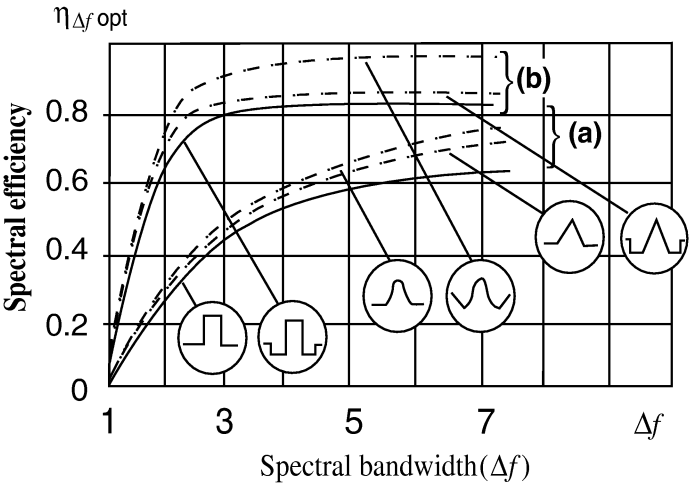


**FIGURE 1.11** Single-polarity video pulses have low-frequency components that do not radiate well through antennas, as shown for cases (a). Correcting the pulse shape to eliminate the low frequencies will increase the spectral efficiency and provide better performance, as shown in (b).

in the summation spectrum $S_\Sigma(f) = S_1(f) - S_2(t)$, the low-frequency components for $f < f_{min}$ were considerably smaller than in the basic spectrum $S_1(f)$, and, for $f > f_{min}$, the changes were insignificant. The corrected bipolar sounding pulse will be

$$u_\Sigma(t) = u_1(t) - u_2(t)$$

Now the spectral efficiency will depend on the parameters of basic and correcting pulse.

The possible maximum values of the spectral efficiency $\eta_{\Delta fopt}$ have been determined for the simplest corrected pulses, consisting of the difference between two single-polarity pulses, each of which has a simple waveform of rectangular, bell-shaped, or triangular.

The dependencies of $\eta_{\Delta fopt}$ on $\Delta f$, computed for different forms of the basic and correcting pulses, are shown in curve (b) of Figure 1.11. The introduction of a corrected pulse appreciably improved the radar efficiency.

Figure 1.12 gives the curves indicating the dependence of the ratio of the maximum spectral efficiency of the pulses with the correction and without correction $\eta_{\Delta fopt(with\ corr)}/\eta_{\Delta fopt(without\ corr)}$ on the signal spectrum $\Delta f$. These curves make it possible to estimate the effectiveness of correction of the pulse form so as to increase the spectral efficiency. With the growth of $\Delta f$, the correction of the pulse form becomes less effective, decreasing from 2 at $\Delta f = 3$ down to 1.2 at $\Delta f = 10$.

In the general case, the correcting pulse $u_2(t)$ can be shifted relative to the basic pulse by the time $t_0$. Then it can be written that

$$u_\Sigma(t) = u_1(t) - u_2(t - t_0)$$

and we shall get for the summary spectrum

$$S_\Sigma(f) = [S_1^2(f) - 2S_1(f)S_2(f)\cos 2\pi f t_0 + S_2^2(f)]^{\frac{1}{2}}$$

Figure 1.13 shows the dependence of the maximum spectral efficiency $\eta_{\Delta fopt}$ on the relative delay $\gamma = t_0/\tau$ and the correcting pulses of different forms on the basic rectangular pulse. Curves (a)

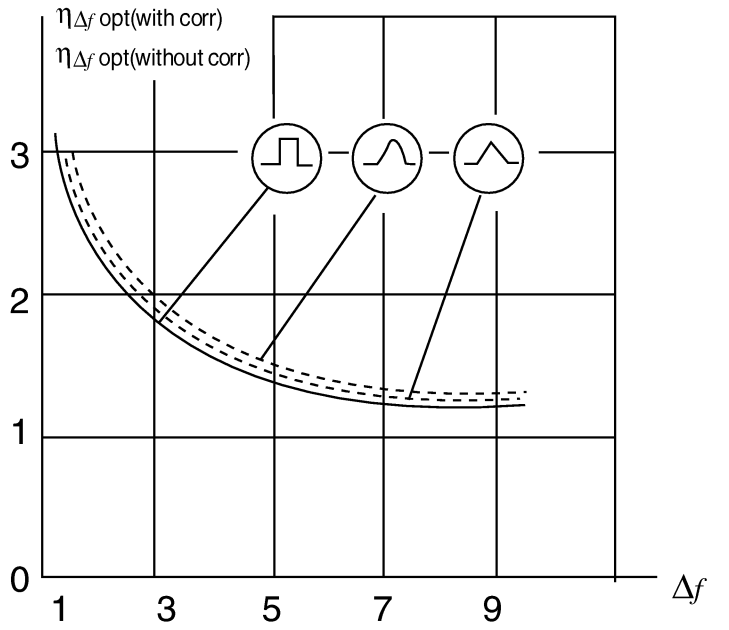


**FIGURE 1.12** The dependence of the spectral efficiency of pulses with and without corrections to the signal spectrum.

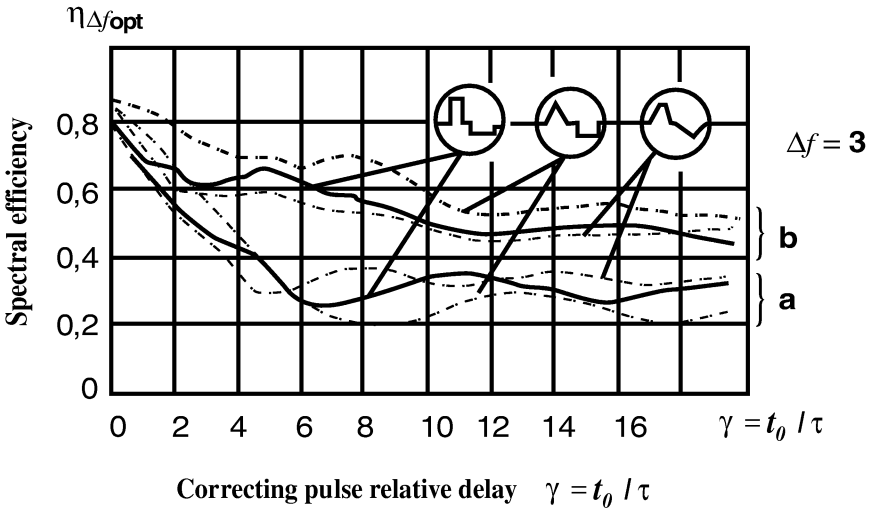


**FIGURE 1.13** Shifting the correcting pulse by some time increment can improve the system's performance. This plot shows the effects of the relative time delay on spectral efficiency.

reflect the dependence on $\eta_{\Delta fopt}$ on the delay $\gamma$ at the constant parameters of correction. Curves (b) in Figure 1.13 reflect the same dependence for the case where optimal correction parameters were sought for each value of $\gamma$.

From a practical point of view, the greatest interest will be the corrected pulses, whose basic and correcting pulses do not overlap by time, i.e., when $t_0 > (\tau_1/2 + \tau_2/2)$. For the case $\gamma > 1.5$, the

pulses follow each other, and $\eta_{\Delta fopt}$ becomes less than at $\gamma = 0$ but remains higher than in the uncorrected pulse case.

Thus, when selecting video pulse UWB radar waveforms, it is necessary to take into account the spectral efficiency because, for the singe-polarity pulses, it can be considerably less than 1. This is especially true of the pulses having the ratio of the high spectrum frequency to the lower one equal to $\Delta f < 3$. In this case, the efficiency does not exceed 50 percent.

By increasing $\Delta f$, the spectral efficiency increases so that, at $\Delta f \approx 10$, it can reach 85 to 90%. Therefore, it is advisable to use the correction of sounding pulses at $\Delta f < 3$, which provides higher values of spectral efficiency. The correction of the pulse waveform makes it possible to increase the spectral efficiency at $\Delta f \leq 3$ by two times, and about 1.2 times at $\Delta f \approx 10$.

## REFERENCES


1. Harmuth, H., *Nonsinusoidal Waves for Radar and Radio Communications*. Academic Press, New York, 1981. Translation into Russian. Radio i Svyaz, Moscow, 1985.
2. Harmuth, H., "Radar Equation for Nonsinusoidal Waves." *IEEE Transactions on Electromagnetic Compatibility,* No. 2, v. 31, 1989, pp. 138–147.
3. L. Astanin and A. Kostylev, *Fundamentals of Ultra-Wideband Radar Measurements,* Radio i Svyaz, Moscow, 1989. (Published as *Ultrawideband radar measurements: analysis and processing*, IEE, UK, London, 1997.)
4. Stryukov B., Lukyannikov A., Marinetz A., Feodorov N., "Short impulse radar systems." *Zarubezhnaya radioelectronika* No. 8, 1989, pp. 42–59.
5. Immoreev, I., "Use of Ultra-Wideband Location in Air Defence." *Questions of Special Radio Electronics. Radiolocation Engineering Series*. Issue 22, 1991, pp. 76–83.
6. Immoreev, I. and Zivlin, V., "Moving Target Indication in Radars with the Ultra-Wideband Sounding Signal." *Questions of Radio Electronics, Radiolocation Engineering Series*, Issue 3, 1992.
7. Shubert, K. and Ruck, G., "Canonical Representation of Radar Range Equation in the Time Domain."*SPIE Proceedings: UWB Radar Conference,* Vol. 1631, 1992.
8. Immoreev, I. and Vovshin, B., "Radar observation using the Ultra Wide Band Signals (UWBS)," International Conference on Radar, Paris, 3–6 May, 1994.
9. Immoreev, I. and Vovshin, B., "Features of Ultrawideband Radar Projecting." IEEE International Radar Conference, Washington, May, 1995.
10. Immoreev, I., Grinev, A., Vovshin B., and Voronin, E., "Processing of the Signals in UWB Videopulse Underground Radars," International Conference, Progress in Electromagnetions Research Symposium. Washington, DC, 22–28 July, 1995.
11. James D. Taylor (ed.), *Introduction to Ultra-Wideband Radar Systems*. CRC Press, Boca Raton, FL, 1995.
12. Osipov M., "UWB radar," *Radiotechnica*, No. 3, 1995, pp. 3–6.
13. Bunkin B. and Kashin V. "The distinctive features, problems and perspectives of subnanosecond video pulses of radar systems." *Radiotechnica*, No. 4–5, 1995, pp. 128–133.
14. Immoreev, I., "Ultrawideband (UWB) Radar Observation: Signal Generation, Radiation and Processing." European Conference on Synthetic Aperture Radar, Konigswinter, Germany, 26–28 March, 1996.
15. Immoreev, I., "Ultrawideband Location: Main Features and Differences from Common Radiolocation," *Electromagnetic Waves and Electronic Systems*. Vol. 2, No. 1, 1997, pp. 81–88.
16. Immoreev I. and Teliatnikov L. "Efficiency of sounding pulse energy application in ultrawideband radar." *Radiotechnica*, No. 9, 1997, pp. 37–48.
17. Immoreev, I. and Fedotov, D. "Optimum processing of radar signals with unknown parameters," *Radiotechnica*, No. 10, 1998, pp. 84–88.
18. Immoreev, I., "Ultra-wideband radars: New opportunities, unusual problems, system features," *Bulletin of the Moscow State Technical University*, No. 4, 1998, pp. 25–56.

# 2 Feature Detection in UWB Radar Signals

*Igor I. Immoreev*

## CONTENTS



## 2.1 INTRODUCTION

Any radar signal scattered by a target is a source of target information. However, the returned scattered signal will combine with radar receiver front-end internal noise and interference signals. Each signal processing system must provide the optimal way to extract desired target information from the mixed signal, noise, and interference input. *Optimum* is a term relative to the radar system's mission or function. What is optimal for one use will not be so for another.

Information quality depends on the process that determines the algorithm for analyzing the mixture of signal, noise, and interference and sets the rules for decisions after the analysis is complete. This decision may be based on the detection of the echo signal, the value of the measured signal parameters such as the Doppler shift, power spectral content, or other criteria. The algorithm process efficiency is defined by the statistical criterion, which helps to determine if this algorithm is the best possible one for the application. An algorithm is called the optimum if the information is extracted in the best way for a particular purpose, and the resulting distortions of information resulting from processing operations are minimal.

Radar functional requirements will determine the sophistication of the signal processing algorithms. Simple binary detection provides minimal information and shows only that some target is present. Distinguishing and resolving several targets requires additional information requirements and therefore a larger signal bandwidth. If the signal parameters are time variable, the quantity of the information received must be large enough for the recovery of echo signals. Sophisticated applications such as target imaging and recognition will require even more information.

For passing information, the channel frequency bandwidth and the signal bandwidth are the determining factors. An advanced "smart" radar that can resolve multiple targets in a small space, or image and identify targets, will need a wider bandwidth signal than other systems. Target information begins with target detection. Therefore, primary attention will be given to this problem in this chapter.

0-8493-4267-8/01/$0.00+$.50

Barton, Skolnik, Shirman, Sosulin, Gutkin, and others have described the problems of detection for targets concealed by noise in Refs. 1 through 5. The problem is that past work was done mainly for narrowband signals, i.e., sinusoidal and quasi-sinusoidal signals. Mathematical treatment of sinusoidal signals is simplified, because they do not change their waveforms during the processing operations of summation, subtraction, differentiation, and integration, which occur during radiation, reflection from the target, and reception at the radar receiver. In this case, we mean that the signal amplitude, frequency, and initial phase of narrowband echo signals can change. Target reflection can modulate any of the signal parameters, but the shape of narrowband signals is unchanged during target location and remains a sinusoidal harmonic oscillation. For narrowband signal and target detection, the known signal waveform is *a priori* information. This feature allows using matched filters and correlators to process narrowband radar signals.

In the case of high-information-content ultra-wideband (UWB) radar signals, not only the signal parameters but also the signal shape will change during processing operations mentioned above. As shown in Refs. 6 and 7, the UWB signal changes shape during target locating many times. As a result, the shape of a signal at the processor input differs essentially from the shape of a radiated signal. The changed signal waveform contains target information, as shown by Van Blaricum and Sheby in Ref. 6. As a result, conventional optimal processing methods, such as matched filtering and signal correlation, are impossible to implement, because there is no *a priori* signal waveform information.

Building successful UWB radars will require new processing algorithms. The objective of UWB radar optimal processing algorithms should be to give the maximum signal-to-noise ratio at the processor output for signals with unknown shape. To solve this problem, first we consider the conventional narrowband signal processing algorithms in Section 2.2 then examine quasi-optimal and optimal detection methods for UWB signals in Sections 2.3 and 2.4.

## 2.2 BRIEF OVERVIEW OF CONVENTIONAL METHODS FOR OPTIMAL DETECTION OF RADAR SIGNALS

The majority of radar target detection prediction problems can be solved using the methods of statistical decision theory. Those methods analyze the receiver output voltage during a certain period of time and reach a decision about whether a target return signal is present or absent in the voltage. Because the signal must be described statistically, the quality of detection is expressed as the probability of detection and false alarm for given target conditions. Two conditions should be met to make a reliable target detection decision.

First, we must have some preliminary *(a priori)* information about the constituents of receiver output voltage. A well known noise probability density $W_0(u)$ and signal + noise probability density $W_1(u)$ can be used as *a priori* information. Later, we will show that the shape of a desired signal can be also used as *a priori* information.

Second, the output voltage processing and target presence detection must be performed according the particular algorithm. This process must increase the volume of the received *(a posteriori)* information on the constituents of output voltage to the maximum. Furthermore, we consider this algorithm. We can have two groups of events for binary detection.

The first group comprises two events, which reflect the actual situation in the radar surveillance area. They are event $A_1$, when the target is present, and event $A_0$, when the target is absent. Each of these two events has a probability of occurrence described by integrated distribution functions $P(A_1)$ and $P(A_0)$. These events form a full group and are incompatible, because only one of them may happen at a time; therefore, $P(A_1) + P(A_0) = 1$.

The second group is another two events, which reflect the actual situation at the signal processor output after the received voltage has been processed and the decision has been made. These two events are $A'_1$, meaning that the target is present, and event $A'_0$, meaning the target is absent. The

probabilities of occurrence of these two events are $P(A'_1)$ and $P(A'_0)$. These events are incompatible, so they too form a full group $P(A'_1) + P(A'_0) = 1$.

One event of the first group and one event of the second group will be noted in every surveillance area cell when detecting a target. As a result, only one of four possible variations of simultaneous occurrence of two independent events appears in every volume cell. Two of these variants apply to the true case so that the events $A_1$ and $A'_1$ correspond to reliable target detection, and the events $A_0$ and $A'_0$ correspond to the case when targets are not detected because none is there. Another two variants are wrong decisions cases where the events $A_1$ and $A'_0$ correspond to the miss of a target and the events $A_0$ and $A'_1$ correspond to a false alarm where no target is present, but one is indicated. These wrong case variants result from the statistical (noise) characteristics of the receiver output voltage.

As is known, the probability of a simultaneous occurrence of two compatible and dependent events $P(A_n + A'_k)$ is determined by the multiplication of probabilities. It is equal to the product of the probability of one even $P(A_n)$ and the conditional probability of the occurrence of the second event calculated under the assumption that the first event has already occurred $P(A'_k/A_n)$:

$$P(A_n + A'_k) = P(A_n) \cdot P(A'_k/A_n) \tag{2.1}$$

As shown in Figure 2.1, the conditional probability of false alarm, given the condition that the signal is absent, is the probability that noise voltage $u(t)$ will exceed the threshold value $u_0$.

$$P(A'_1|A_0) = P[u(t) \geq u_0] = \int_{u_0}^{\infty} W_0(u)du \tag{2.2}$$

Then the probability of false alarm is

$$P(A_0 + A'_1) = P(A_0) \cdot P(A'_1|A_0) = P(A_0)\int_{u_0}^{\infty} W_0(u)du \tag{2.3}$$

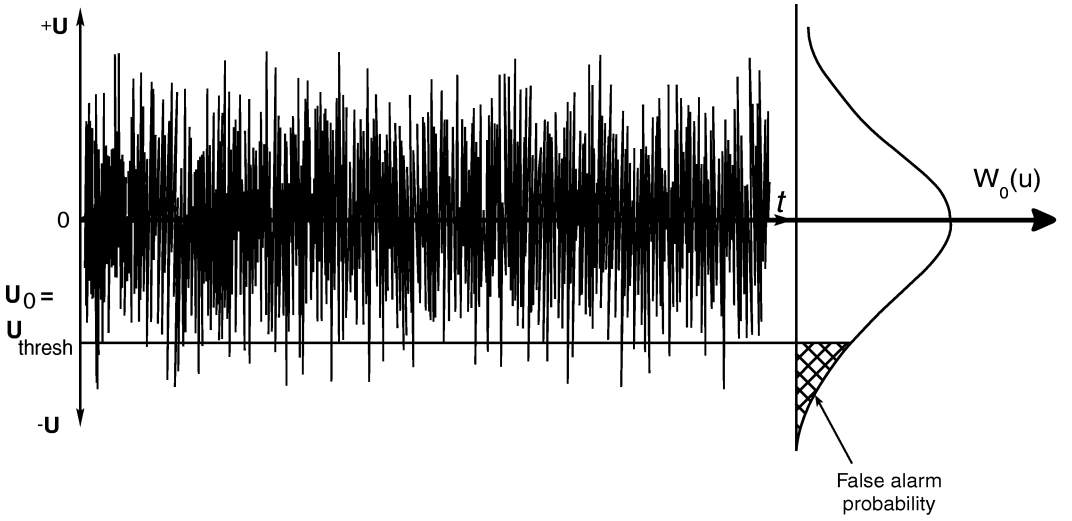


**FIGURE 2.1** False alarm probability for random noise, or the chance that random noise will exceed some threshold value.

Figure 2.2 shows the conditional probability that the signal will be missed when it is present, or the probability that the signal + noise voltage *u(t)* will not exceed the threshold value $u_0$:

$$P(A'_0|A_1) = P[u(t) \le u_0] = \int_0^{u_0} W_1(u)du \tag{2.4}$$

The probability that the desired signal will be missed is determined by the following expression:

$$P(A_1 + A'_0) = P(A_1) \cdot P(A'_0|A_1) = P(A_1)\int_0^{u_0} W_1(u)du \tag{2.5}$$

The events $(A_0 + A'_1)$ and $(A_1 + A'_0)$ are incompatible. In accordance with the rule of composition of probabilities, the probability that one of two wrong decisions will be made is

$$\begin{aligned} P[(A_0 + A'_0) \text{ or } (A_1 + A'_0)] &= P(A_0 + A'_1) + P(A_1 + A'_0) \\ &= P(A_0)\int_{u_0}^{\infty} W_0(u)du + P(A_1)\int_0^{u_0} W_1(u)du \end{aligned} \tag{2.6}$$

If we change the limits of integration, this expression will take the following form:

$$P[(A_0 + A'_1) \text{ or } (A_1 + A'_0)] = 1 - \left[P(A_0)\int_0^{u_0} W_0(u)du + P(A_1)\int_{u_0}^{\infty} W_1(u)du\right] \tag{2.7}$$

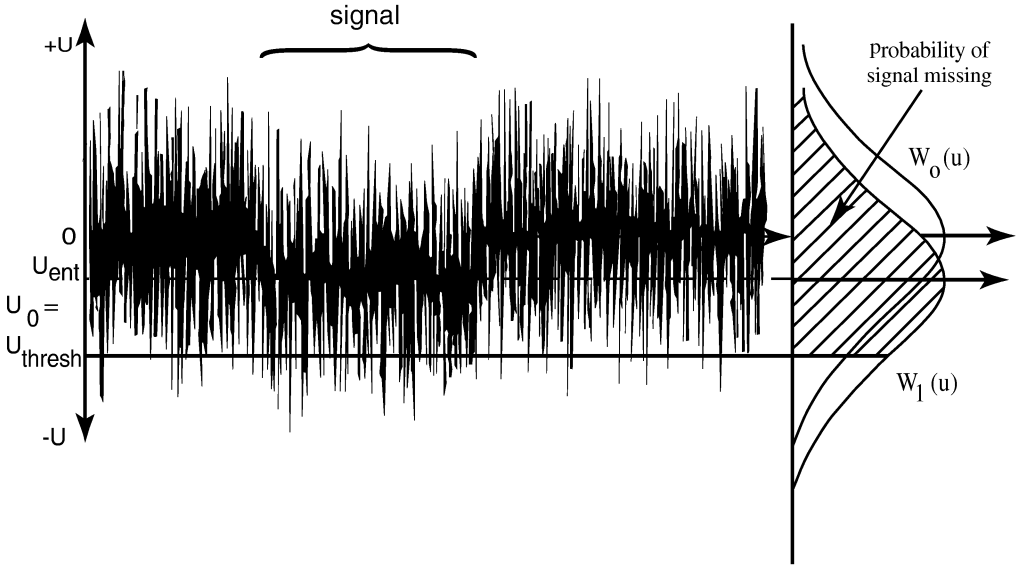


**FIGURE 2.2** Conditional probability that the signal will not be detected when present, or the probability that the signal plus noise voltage *u(t)* will not exceed the threshold $u_0$.

The probability of making true decision will be

$$P[(A_0 + A'_0) \text{ or } (A_1 + A'_1)] = 1 - [P(A_0 + A'_1) \text{ or } (A_1 + A'_0)]$$
$$= P(A_0)\int_0^{u_0} W_0(u)\mathrm{du} + P(A_1)\int_{u_0}^{\infty} W_1(u)du \tag{2.8}$$

To find the optimum threshold level $u_0$, it is necessary to determine threshold value for which the probability of making true decision is maximum. For this purpose, we calculate the following derivative:

$$\frac{dP[(A_0 + A'_0) + (A_1 + A'_1)]}{du_0} \tag{2.9}$$

and then set it to zero.

As a result, we get $P(A_0)W_0(u_0) = P(A_1)W_1(u_0)$ or

$$\frac{W_1(u_0)}{W_0(u_0)} = \frac{P(A_0)}{P(A_1)} \tag{2.10}$$

Figure 2.3 shows the noise probability density $W_0(u)$ and the signal + noise probability density $W_1(u)$. It is evident from the picture that, the larger the signal amplitude, the higher the threshold level must be. For $P(A_0) = P(A_1) = 0.5$, the optimum threshold level is defined by the point of crossing of two probability density $W_0(u)$ and $W_1(u)$. The necessary condition for making the decision on target presence is

$$\frac{W_1(u)}{W_0(u)} \geq \frac{P(A_0)}{P(A_1)} \tag{2.11}$$

We can make a decision on target absence by reversing the inequality.

This inequality is true for the value of the noise voltage and the signal plus noise voltage in one moment of time, and it comprises a one-dimensional probability density $W_0(u)$ and $W_1(u)$. The inequality can be extended to the case where the decision is made from $N$ voltage values, which

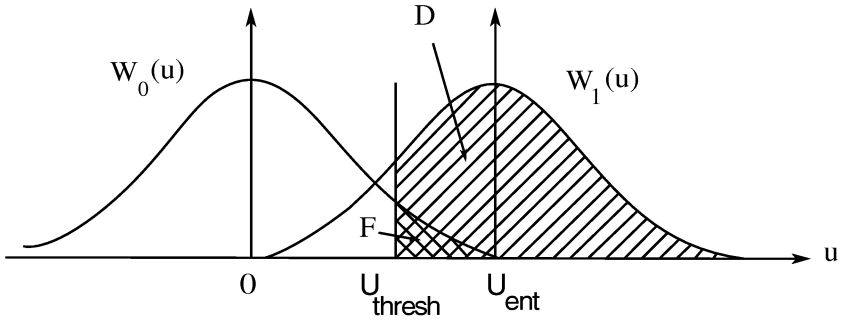


**FIGURE 2.3** The noise distribution function $W_0(u)$ and the signal plus noise distribution function $W_1(u)$.

we can get from the ensemble of realization at one time moment or from one realization at different time moments:

$$\frac{W_1(u_1, u_2, u_3,\ldots, u_N)}{W_0(u_1, u_2, u_3,\ldots, u_N)} \geq \frac{P(A_0)}{P(A_1)} \tag{2.12}$$

In this case, the probability density $W_0$ and $W_1$ become multidimensional.

This most simple statistical criterion is called the *ideal observer criterion.* In practical cases, the disadvantage of this criterion is that we do not know the *a priori* probability $P(A_1)$ that a desired target is present, and the probability $P(A_0)$ that a desired target is not in the radar surveillance area. There is one further problem in that the ideal observer criterion does not consider the consequences of wrong decisions.

To overcome the ideal observer criterion, we introduce weight coefficients $B$ and $C$ in the equation, which describes the estimation of probability of wrong decisions. These coefficients characterize the losses caused by false alarm and target miss:

$$P[(A_0 + A'_1) or\ (A_1 + A'_0)] = B \cdot P(A_0 + A'_1) + C \cdot P(A_1 + A'_0) \tag{2.13}$$

In this case, the following inequality must be satisfied to make a decision on the target presence:

$$\frac{W_1(u_1, u_2, u_3,\ldots, u_N)}{W_0(u_1, u_2, u_3,\ldots, u_N)} \geq \frac{B \cdot P(A_0)}{C \cdot P(A_1)} \tag{2.14}$$

This statistical criterion is called the *minimum risk criterion.* Its practical implementation is rather difficult, not only because the priori probabilities $P(A_1)$ and $P(A_0)$ are unknown, but also because the *a priori* estimations of weight coefficients $B$ and $C$ are unknown as well. This criterion, along with the ideal observer criterion, is referred to as the *Bayes criterion.*

One more well known criterion is the *maximum likelihood criterion.* The probability density for $N$ random voltage values at the receiver output $W(u_1, u_2, u_3,\ldots, u_N)$, which we mentioned above, is named the *likelihood function.* The maximum likelihood method helps to determine the maximum value of this function. To perform this operation, we must take the derivative of the likelihood function with respect to the desired signal and set it to zero. The solution of this equation helps to find the maximum likelihood estimation of the signal. For example, if random values of voltage at the receiver output: $u_1, u_2, u_3,\ldots, u_N$ are distributed normally, the estimation is equal to their average value. This method gives less dispersed estimations than other methods. Such estimations are called *efficient,* so the criterion of the optimum operations, which use the maximum likelihood method, is the estimation efficiency. If the maximum likelihood criterion is used, then the decision on target presence is made when the likelihood function $W_1$ exceeds the likelihood function $W_0$:

$$\frac{W_1(u_1, u_2, u_3,\ldots, u_N)}{W_0(u_1, u_2, u_3,\ldots, u_N)} \geq 1 \tag{2.15}$$

As was mentioned above, we need some *a priori* probabilities for making decisions on target presence, but in many practical cases these will be unknown. Another widely used criterion, which does not depend on these probabilities, is called the Neumann–Pearson criterion. This provides the maximum probability of detection $D = P(A_1 + A'_1)$, at the constant false alarm rate $F = P(A_0 +$

$A'_1$). According to this criterion, the threshold value $u_0$ located in the right part of the likelihood expression is chosen for a given conditional probability of false alarm:

$$P[u(t) \geq u_0] = \int_{u_o}^{\infty} W_0(u)du \tag{2.16}$$

So, in many cases, the solution of the problem of target detection is reduced to the calculation of the following ratio:

$$\Lambda = \frac{W_1(u_1, u_2, u_3,\ldots, u_N)}{W_0(u_1, u_2, u_3,\ldots, u_N)} \tag{2.17}$$

This ratio is called the *likelihood ratio.* We make a decision on target presence when this ratio exceeds some constant level $u_0$, given according to the selected criterion.

The calculation of the likelihood ratio helps to design the optimum receiver. Conventional methods for optimal radar signal detection use the noise probability density at the receiver output as *a priori* information. This noise is usually approximated by so called *white noise,* which has an equally distributed spectral power density $N_0$ (W/Hz) within the receiver bandwidth $\Delta f$ and the normal time probability density of the voltage $u$:

$$W_0(u) = \frac{1}{\sqrt{2\pi\sigma}}\exp\left(-\frac{u^2}{2\sigma^2}\right) \tag{2.18}$$

This probability density has zero average value, and its dispersion is $\sigma^2 = N_0\Delta f$. The samples of noise voltage are statistically independent if they are spaced at the $\Delta t = 1/2\Delta f$. Then, the likelihood function for $N$ noise samples is the product of $N$ factors so that

$$W_0(u_1, u_2, u_3,\ldots, u_N) = \prod_{i=0}^{N} W_0(u_i) = \left(\frac{1}{\sqrt{2\pi\sigma}}\right)^N \exp\left(-\frac{1}{2\sigma^2}\sum_{i=1}^{N} u_i^2\right) \tag{2.19}$$

The probability density for signal plus noise depends on a signal structure. We usually use a hypothetical signal to understand the general laws of optimal processing in the conventional radar theory. For this case, all the signal parameters are fully known except the time of arrival. Therefore, the signal plus noise probability density differs from the noise probability density only by a nonzero average value that is equal to the signal amplitude.

$$W_1(u) = \frac{1}{\sqrt{2\pi\sigma}}\exp\left(-\frac{(u-s)^2}{2\sigma^2}\right) \tag{2.20}$$

The likelihood function for the signal plus noise is

$$W_1(u_1, u_2, u_3,\ldots, u_N) = \prod_{i=0}^{N} W_1(u_i) = \left(\frac{1}{\sqrt{2\pi\sigma}}\right)^N \exp\left[-\frac{1}{2\sigma^2}\sum_{i=1}^{N}(u_i - S_i)^2\right] \tag{2.21}$$